RF sources and LLRF system

1. Abstract

RF sources are widely used for the beam acceleration. High power radio frequency (HPRF) devices such as klystron will be summarized. Recently, digital low-level radio-frequency (LLRF) control becomes popular (especially for the control of superconducting cavities). System configuration and RF performance with this digital LLRF will be also presented.

2. Introduction of RF system

In an accelerator, RF system will provide the accelerating energy for the charged beam current. It is a system intended to transfer energy to beam of charged particles by interaction with electric field oscillating at RF frequency [1][2].

2.1. Why RF ?

First of all, we rise a question spontaneously. Why we does not use the simplest method for beam acceleration? For instance, applying an electrostatic field as shown in Fig. 1 to accelerate a charged beam. In order to produce higher energy beam current, the value of the DC voltage, V_c, becomes higher and higher; however, if the high voltage V_c exceed some threshold, the electrical breakdown happens; as a result, the energy gain of this electrostatic field structure is limited to few MeV [1].

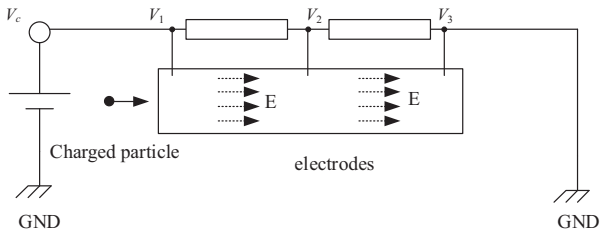

Fig. 1: Electrostatic field acceleration

In the case of the radio frequency RF acceleration as shown in Fig. 2. The electric field has reversed polarities in consecutive gaps.

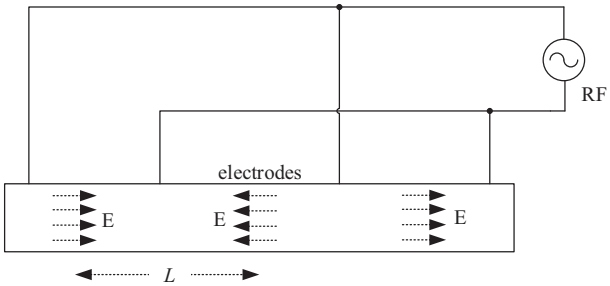

Fig. 2: Radio frequency acceleration

If the synchronism condition

$$L = \frac{vT_{RF}}{2} \qquad (2\text{-}1)$$

is fulfilled, where v is the velocity of the particle, L is the distance between consecutive gaps, and T_{RF} the RF period, then for the given voltage V_{RF}, all the gaps will accelerate the particles and provide energy [1].

2.2. Components of RF system

As mentioned above, the RF system will transfer the energy to the charged beam current, but where is this initial energy derived from at the very beginning and how does the energy (or power) finally transfer to the charged beam current? Fig. 3 illustrates the energy transfer process in an RF system. Generally, the energy (or power) is transferred to beam by three steps [2].

- The transformation of the alternating current (AC) power from transmission network (50~60 Hz, 100 V~240 V) to direct current (DC) power (high voltage, e.g. 100 kV) that take place in a power converter
- The transformation of the DC power into radio frequency power (high power, and high frequency, e.g. 1 MW and 1.3 GHz).

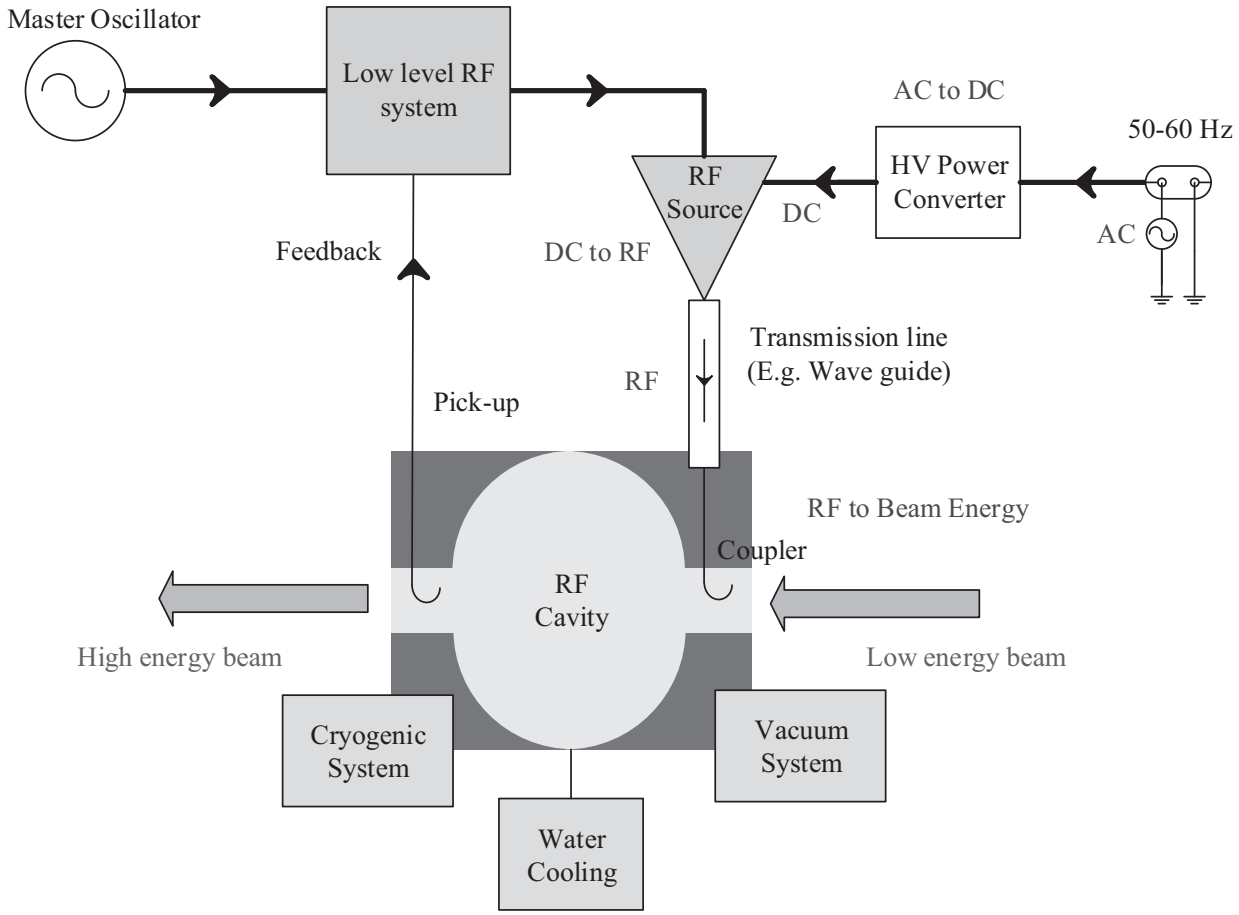

Fig. 3: Block diagram of an RF system in accelerator

This transformation takes place in RF sources.

- The transformation from the RF power to a charged particle beams that occurs in the gap of an accelerating cavity. The beam will gain (or lose) energy from the RF field in the cavity.

These three steps of the energy transmission covers the three main components of the RF system which are, the HV power converter (or HV power supply), the RF source (or RF amplifier), and the RF cavity. Furthermore, we need a control devices (LLRF) to regulate the RF cavity and RF sources. We also need a transmission line (waveguide) to transfer the RF power from RF source side to the RF cavity side with minimum loss and zero reflection. We need a RF coupler to inject the power from the transmission line to the RF cavity. In addition, if the cavity is a super-conducting cavity, we need some auxiliary system, such as vacuum, water cooling, and cryogenic system [2].

The main features of the components in an RF system is shown in Table 1. In this lecture, we will mainly focus on the RF sources and LLRF feedback control systems.

3. RF sources

As discussed above, the RF source will provide the RF power for the cavity by extracting the energy from the high voltage power converter (DC power). There are various types of RF sources with different principle, efficiency and applicability. The two main categories are solid state equipment like solid state amplifier (SSA) and vacuum tubes such as

Table 1 Components of RF system

Elements	Main function	Features
Power Convertor	AC power to DC power	Rectifier + HV transformer + energy storage Pulsed power convertor is also named Modulator.
RF source	DC power to RF power	The conversion takes place by means of an electron beam accelerated by the DC voltage and density modulated at the RF frequency by a grid (vacuum tube), by a cavity (klystron), or directly by an applied voltage (transistor). The modulated RF power is then extracted from a resonant cavity excited by the electron beam.
RF cavity	RF power to beam Energy	Concentrate the RF energy under the form of electric field on a gap, with minimum power loss.
LLRF	Stabilize the RF field	Stabilizing the cavity voltage against disturbances coming from RF source, RF convertor, the RF cavity, or the charged beam current, and minimizing the cavity input power with some tuning system. The LLRF system is usually a set of electron devices, with the development of digital technique, digital LLRF system become main stream.
Transmission line	Transport the RF power to the RF cavity	Transport the power from RF source to the accelerating cavity without reflection and loss (E.g. usually waveguide and coaxial).
Coupler	Inject the power from transmission line to the RF cavity	Coupling the transmission line to the field distribution in the cavity.

tetrode, klystron, and induced output tube (IOT) In the cERL at KEK, we have applied klystron, SSA, and IOT as the RF sources. In the followed paper, we will mainly focus on these three RF sources [4-8].

3.1. Solid state amplifier

A solid state amplifier (SSA) mainly consists of an power splitter, amplifier modules and power combiner. The schematic of SSA is illustrated in Fig. 4 [2-4]. Clearly, the RF power is obtained by summing power output of multiple devices by power splitter and combiners. The total output power depends each amplifier's power and the number of the amplifiers. For instance, if we have total of 8 amplifiers of 315 w, then we can obtain approximately 2.5 kW output power.

The SSA is has advantages in cost, stability, reliability and effectivity. It is very suitable for applications with lower power level. For example, in the cERL at KEK, the required power for the main linac cavity is not so high because of the energy recovery technique. Therefore, we have installed two SSAs for the main linac cavities..

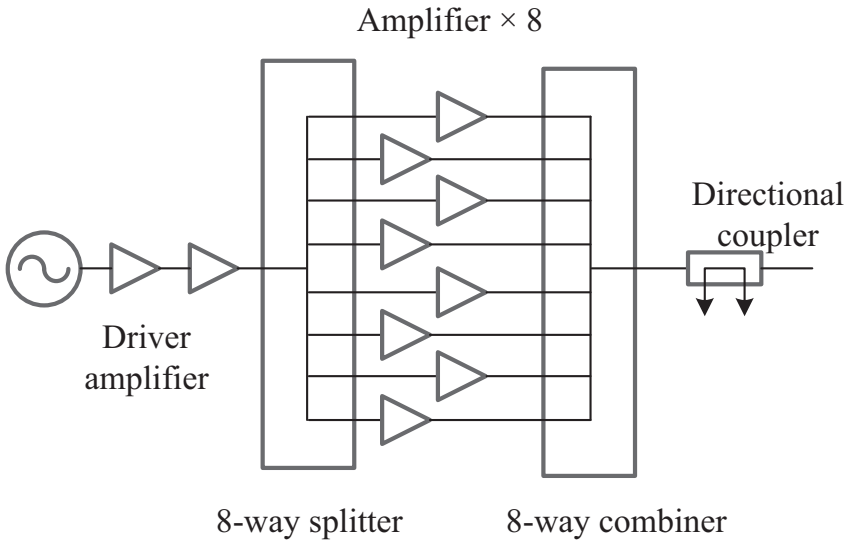

Fig. 4: Block diagram of an solid state amplifier

3.2. Klystron

Klystron is another popular RF sources which can be illustrated in Fig. 5 [5][6]. The electron gun emits the electrons which will be focused on by a low positive voltage on the control grid, thus the electron beams are formed. The beam is then accelerated by a very high DC potential in the accelerator grid and buncher grid. A resonance cavity with a RF input is connected to the buncher grid. The cavity then produce an oscillating electron field that inside buncher cavity. As shown in Fig. 7, the electrons will be accelerated and decelerated because of the effect of the RF field. The butchered electrons is then formed in the drift space when the accelerated electrons overtake the decelerator electrons.

The method to form the bunched electrons is named velocity modulation as shown in the Fig. 6 and Fig. 7. The key-point of this method is to generate a bunched electrons by velocity modulation.

The function of the catcher grid is to extract the energy from the electron beam. It will be placed at the point that the bunched electron is fully formed. The electron bunches will introduce an RF voltage in the grid gap of the catcher cavity. If the placement is appropriate, the catcher cavity will decelerate the bunched beams, since the bunched beam contains the majority of the electrons, the energy will be transferred from the beam to the catcher cavity.

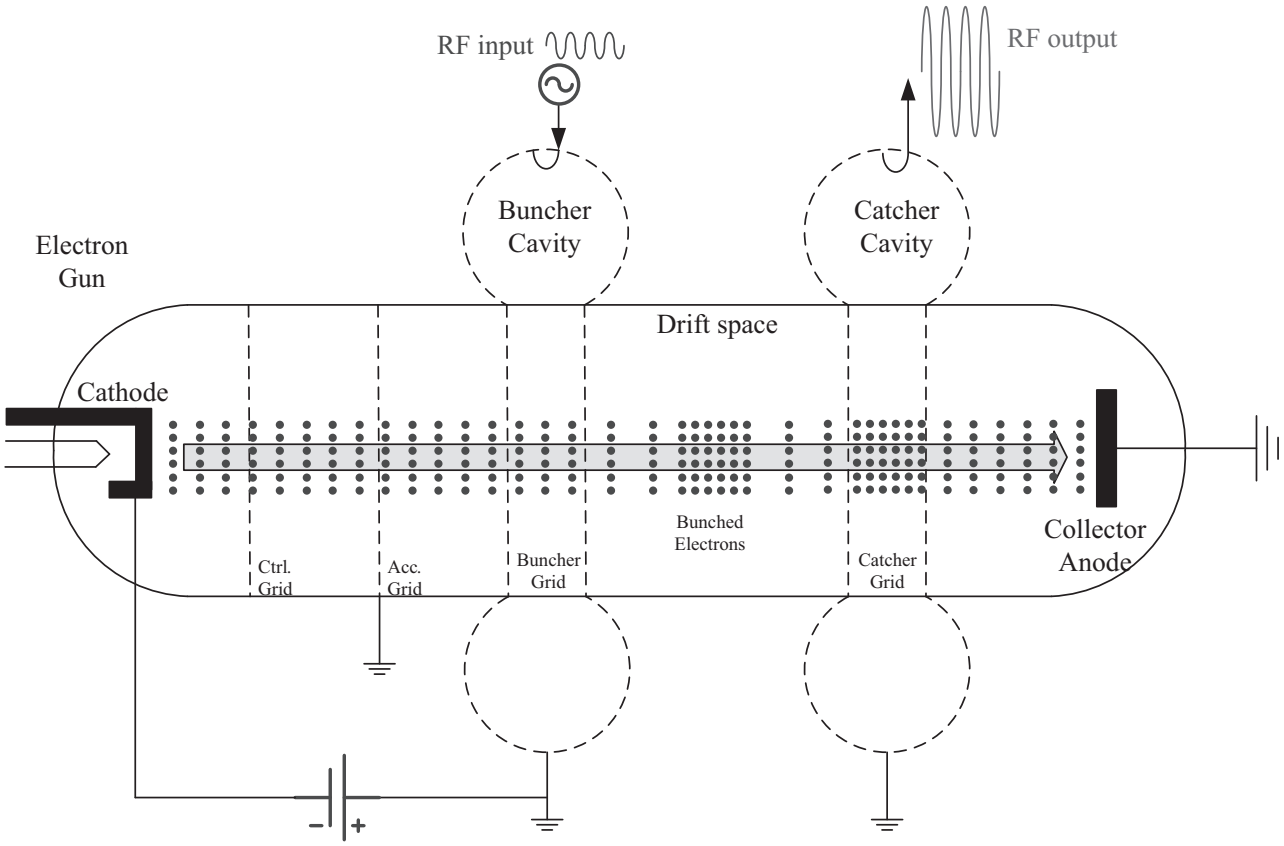

Fig. 5 Schematic of a two cavity klystron

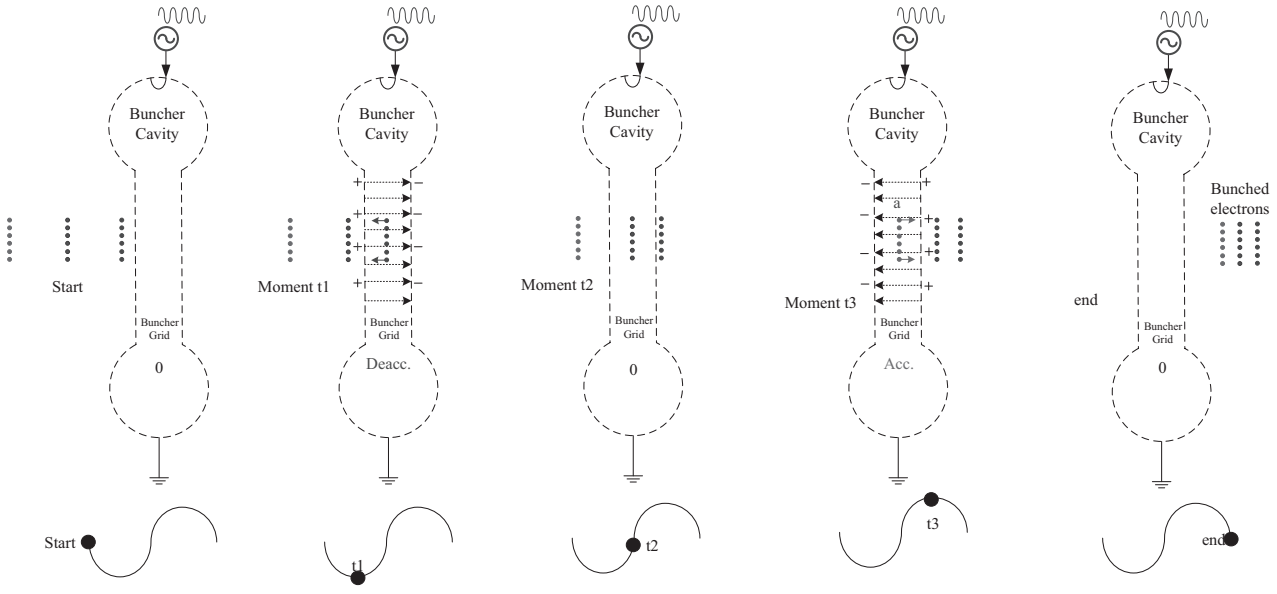

Fig. 6 Buncher cavity action, the formation of the bunched electrons

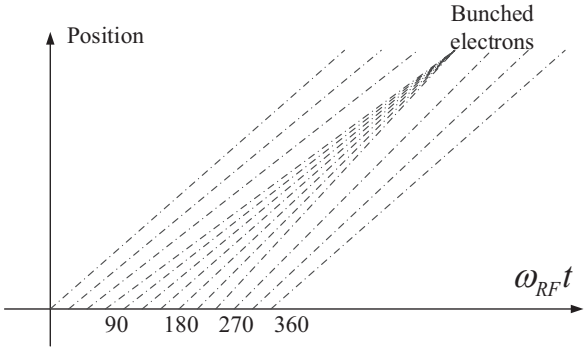

Fig. 7: Diagram showing formation of bunches in a velocity-modulated electron beam.

3.3. IOT

Inductive output tube (IOT) is another RF source which is a combination of coaxial gridded tubes (like tetrode) and klystron, therefore, it is also named Klystrode [7][8]. A schematic of IOT is given in Fig.8. Similar with a tetrode, the IOT also consist of a cathode with a biased control grid, therefore, there is no beam current in the tube except the positive half cycle of the RF input. The electron bunches are then formed and accelerated by the potential between the anode and control grid. In the next step, similar to klystron, the bunched beam will pass through a catcher cavity. This cavity will be excited by the electromagnetic energy if the beam is then extracted.

The main difference between the klystron and IOT is that the method to generate the bunched electrons. In a klystron, this process occurs in the buncher cavity and drift space. The velocity modulation is imposed on the beam current. In the case of the IOT, the bunched electrons is formed within gun religion itself because of the DC bias of the control grid [5].

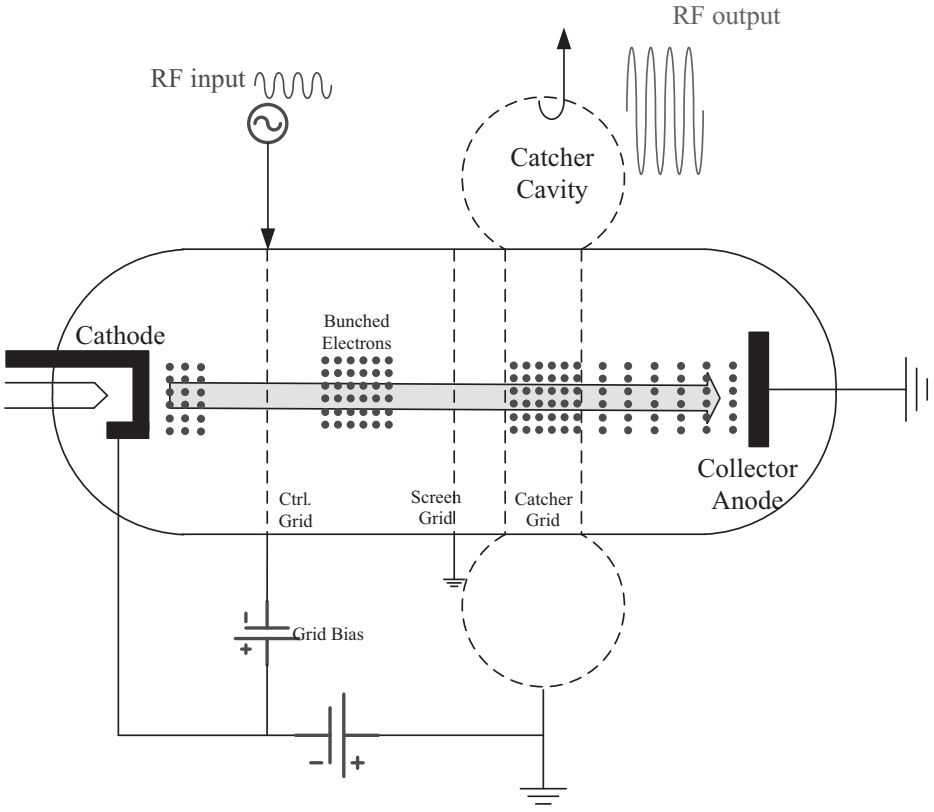

Fig.8 Schematic of IOT

4. RF sources in cERL

A compact energy recovery linac (cERL), which is a test machine for the next generation synchrotron light source 3-GeV ERL, was constructed at KEK. In the cERL, a normal conducting (NC) buncher cavity and three superconducting (SC) two-cell cavities were installed for the injector, and two nine-cell SC cavities were installed for the main linac (ML). The RF sources for each cavity is given in Fig. 9 and Table 2. It should be mentioned that, we only use one klystron to drive the cavities in both of the injector 2 and the injector 3, this is so called vector-sum control [9].

Table 2 Parameters of RF systems at cERL

Cav.	Q_L	RF power [kW]	RF source
Bun.	1.1×10^4	3	8 kW SSA
Inj. 1	1.2×10^6	0.53	25 kW Kly.
Inj. 2	5.8×10^5	2.4	300 kW Kly.
Inj. 3	4.8×10^5		
ML1	1.3×10^7	1.6	16 kW SSA
ML2	1.0×10^7	2	8 kW SSA

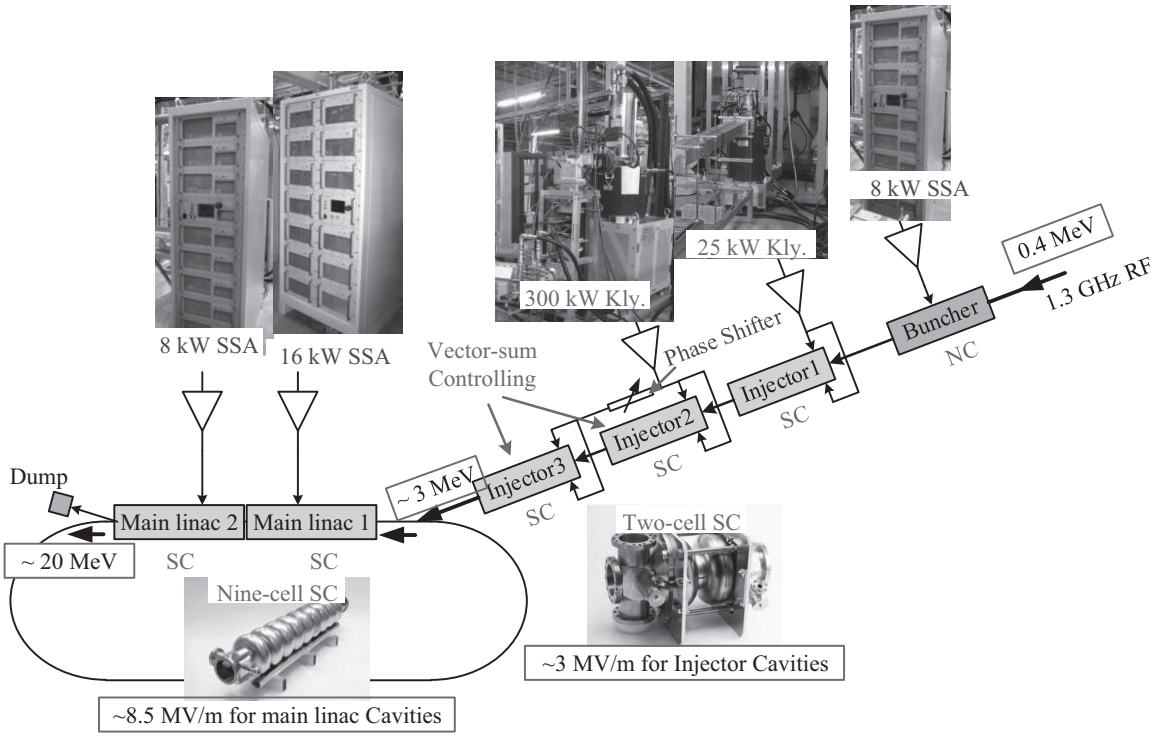

Fig.9 Lay out of RF sources and cavities in cERL at KEK

5. Tutorial of control theory

The LLRF system take charges of stabilizing the RF filed inside the RF cavity. Before we introduce the LLRF system in detail, we would like to discuss the basic issues in a general feedback system. A tutorial including basic definitions and principles in control theory will be presented at first.

5.1. Components of control system

A control system is a device, or set of devices, that manages, commands, directs or regulates the behavior of other devices or systems [10]. Industrial control system are used in industrial production for controlling equipment or machines. As shown in Fig. 10. A control system mainly include a plant, a sensor (or

detector), and a controller. The plant is a system or devices that need to be controlled. The sensor (or detector) is a measuring tool that measured the response of the plant. The controller is a device to regulate or control the behavior of the "plant". The main function of a control system is to maintain some characteristic of the "plant" by applying appropriate sensor and controller.

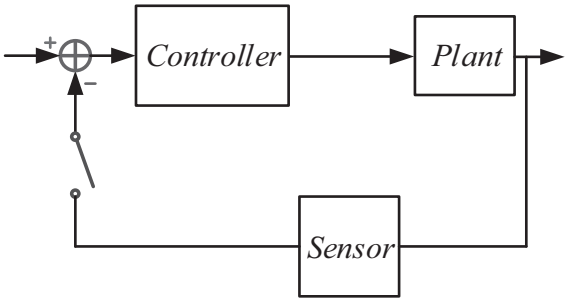

Fig. 10: Components of a control system

5.1.1. Open loop and closed loop

Control system and control theory can be divided two major categories: open loop control and closed loop control.

In an open loop system, the controller (usually feedforward controller) directly drives the plant without any feedback. In a closed-loop system, the current output is taken into consideration and corrections are made based on feedback [10]. A closed loop system is also called a feedback (FB) control system. Fig. 11 has shown the difference between the open loop and closed loop

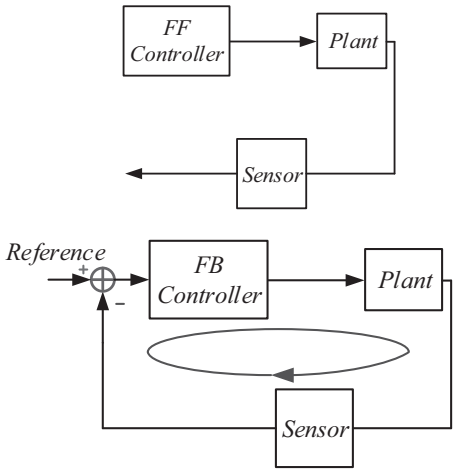

Fig. 11: Open loop vs. closed loop

5.1.2. Transfer function

A transfer function is a ratio of the output of a system to the input of a system. Mathematical representation of a transfer function is given as

$$H(s)=\frac{Y(s)}{X(s)},\ Y(s)=H(s)\cdot X(s). \qquad (5\text{-}1)$$

where the $H(s)$, $Y(s)$ and $X(s)$ represent the Laplace-transform of the system, output signal and input signal, respectively.

The transfer function $H(s)$ includes every information of the system (usually can be seen as a representation of a system model) i.e. if we know the transfer function $H(s)$ of a specified system, we can calculate the output $Y(s)$ by any input $X(s)$.

Takes the cavity model as an instance. The superconducting cavity can be seen as a parallel resonance circuits of resistor, capacitor, and inductor which can be shown in Fig.12.

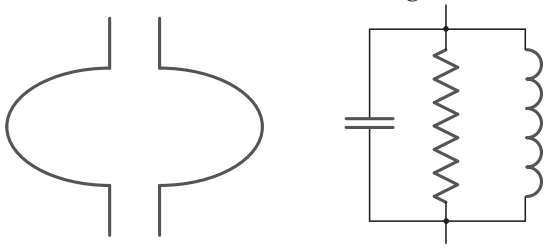

Fig. 12: Cavity equivalent circuits

The impedance (or conductance) of the parallel resonance circuit is given by

$$\frac{1}{Z}=\frac{1}{R}+sC+\frac{1}{Ls}=\frac{Ls+RLCs^2+R}{RLs} \quad and$$

$$Z(s)=\frac{\frac{s}{C}}{s^2+\frac{1}{RC}s+\frac{1}{LC}} \tag{5-2}$$

where the R, L, and C represent the resistance, capacitance and inductance, respectively. Usually, we use quality factor, Q, and resonance radian frequency, ω_0 to replace the R, L and C. Therefore, the transfer function of the cavity model is given by

$$Z(s)=\frac{\frac{s}{C}}{s^2+\frac{1}{RC}s+\omega_0^2}=\frac{\frac{R\omega_0}{Q}s}{s^2+\frac{\omega_0}{Q}s+\omega_0^2} \tag{5-3}$$

where we have $Q=R\sqrt{\frac{C}{L}}, \omega_0=\sqrt{\frac{1}{LC}}$.

5.1.3. Frequency response

Frequency response is a measure of magnitude and place of the output as a function of frequency. We can directly transform the transfer function to frequency response by changing the Laplace notation "s" to Fourier notation "$j\omega$". This process can be expressed by

$$H(s)\big|_{s=j\omega}=H(j\omega)=\left|H(j\omega)\right|e^{j\angle H(j\omega)} \tag{5-4}$$

The significant feature of frequency response is that, we can directly obtain the amplitude and phase response of a specified sinusoidal input by using the frequency response of a system. Since every input signal can be decomposed to a set of sinusoidal signal by Fourier-transform, we can then obtain the corresponding output signal by the frequency response.

The frequency response of a superconducting cavity can be obtained by replace the Laplace notation "s" to Fourier notation "$j\omega$" like

$$Z(s)\big|_{s=j\omega}=\frac{j\frac{\omega_0}{Q}\omega\cdot R}{-\omega^2+\omega_0^2+j\frac{\omega_0}{Q}\omega}=\frac{j\frac{\omega_0}{Q}\cdot R}{-\omega+\frac{\omega_0^2}{\omega}+j\frac{\omega_0}{Q}} \tag{5-5}$$

It is clear to see that, if $\omega=\omega_0$, then we have $Z(j\omega)=R$, that is to say, the cavity is on-resonance, therefore, the parameter, ω_0, is named resonance radian frequency.

5.1.4. Bode plot

Bode plots is a diagram that describe the amplitude-frequency and/or phase-frequency of a system. It is actually a plot of the frequency response H($j\omega$). The bode plot of the cavity bode plot is shown in Fig.13. The quality factor, Q, and resonance frequency, ω_0 are selected to be 1.3×10^6 and 1.3×10^9 Hz.

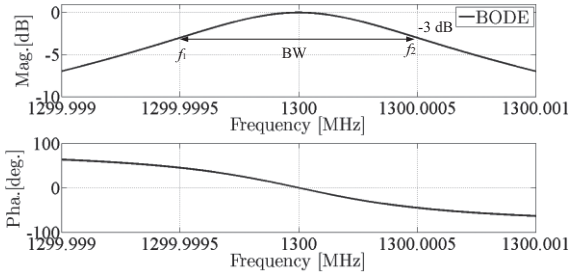

Fig. 13: Bode plots of cavity.

In a Bode plots of the cavity as shown in Fig. 13, we can also define the half power point and 3dB bandwidth. The half power point in a bode plots is that frequency at where the output power has dropped its mid-band value, that is a level of -3 dB. There are two half power point f_1 and f_2 in Fig.13. The 3 dB bandwidth is then defined by the difference between f_1 and f_2. For superconducting cavity, the relationship between Q value and 3dB bandwidth is also given by

$$BW_{3dB} = \frac{f_0}{Q}, f_0 = \frac{\omega_0}{2\pi} \quad (5\text{-}6)$$

5.1.5. Stability Criterial and Gain margin

Stable is the most important issue in a feedback system. We cannot operate a system if it is unstable. There are a lot of stability criterial for a feedback system, such as, root locus method, characteristic equation, routh-hurwitz method and bode plots. In this speech, we only discuss the Bode plots method because it is the most popular and simple criterial. The Bode plot method compares the amplitude-frequency and phase-frequency plots of the system in its open loop as shown in Fig. 14. The stability criterial based on Bode plots can be described as follows.

- Find the frequency where the phase becomes -180 degrees.
- Find the gain, G (in dB) at the same frequency.
- Calculate the gain margin which is defined by 0-G (in dB).
- If the gain margin is larger than 0 dB, the system is stable, or, system is unstable.

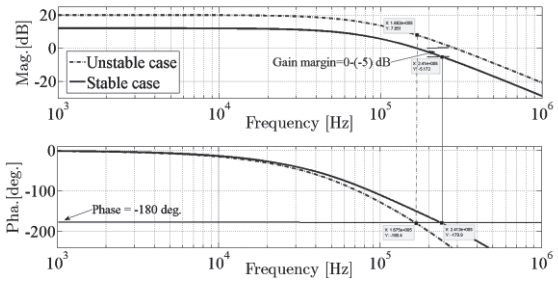

Fig. 14: Gain margin in a Bode plots.

5.2. Analytical study of LLRF system

The analytical study is useful, significant, and essential for a control experts. System model (transfer function) is required in analytical study. Since the LLRF system is actually a FB control system, we would like to set up the system model of a LLRF system as illustrated in Fig. 15.

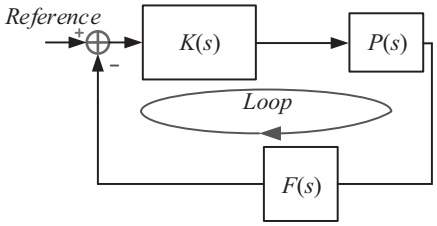

Fig.15: Models of LLRF system

Here $K(s)$, $P(s)$ and $F(s)$ represent the transfer function of controller, plant, and sensor (detector) in baseband, respectively. We would like to discuss each of this models in detail.

The controller P(s) is usually a PI controller in LLRF system. The schematic of a conventional PI controller is given in Fig.16 which holds a transfer function as

$$K(s) = \frac{K_I}{s} + K_P \quad (5\text{-}7)$$

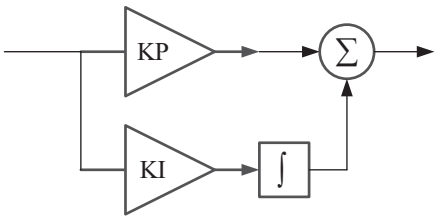

Fig. 16: Structure of PI controller.

The RF cavity is a first order low pass filter in base-band (assume it is operated on-resonance). A cavity with half bandwidth $\omega_{0.5}$ can be expressed by

$$P(s) = \frac{\omega_{0.5}}{s + \omega_{0.5}} \quad (5\text{-}8)$$

The sensor (detector) is also a low pass with a larger bandwidth ω_F which is given by

$$F(s) = \frac{\omega_F}{s + \omega_F} \quad (5\text{-}9)$$

In practice, the dead time exists in the system. The dead time is a time delay that the time after each event during which the system

is not able to record another event (see Fig. 17). The transfer function of a time delay is given by

$$T(s) = e^{-T_d s} \tag{5-10}$$

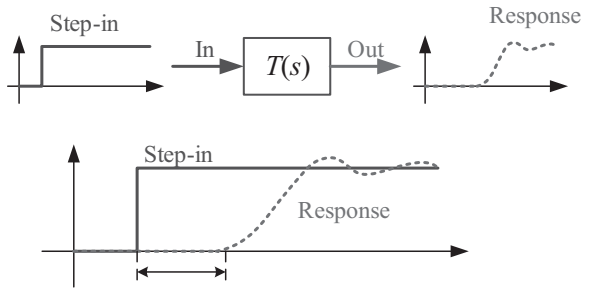

Fig. 17 Dead time in a system.

The overall models of a LLRF system is illustrated in Fig. 18.

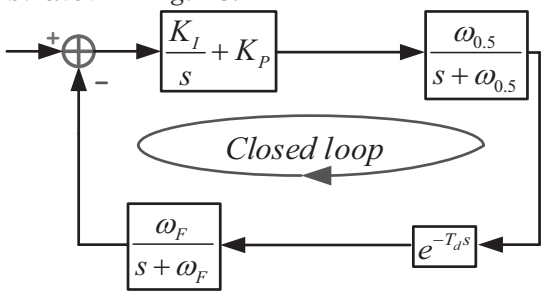

Fig. 18: Overall models of LLRF system including time delay.

The overall open loop diagram is then given by

$$H_{OL}(s) = \left(\frac{K_I + K_P s}{s}\right) \cdot \left(\frac{\omega_{0.5}}{s+\omega_{0.5}}\right) \cdot e^{-T_d s} \cdot \left(\frac{\omega_F}{s+\omega_F}\right) \tag{5-11}$$

Take the buncher cavity as an example, we will analyze its LLRF system based on Fig. 18 and Eq. (5-11). The parameters for the study are given in Table 3

Table 3 Parameters in analytical study

Parameter	Value
$\omega_{0.5}$	93 kHz
K_I	0
K_P	2
T_d	1 μs
ω_F	500 kHz
ML2	1.0×10^7

The Bode plots is then given by Fig. 19. We can then predict the system stability of the LLRF system of the buncher cavity by its Bode plots.

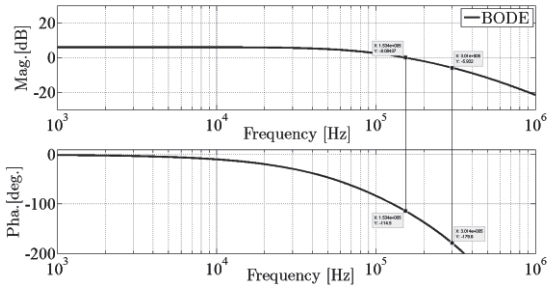

Fig. 19: Bode plots of LLRF system for buncher cavity.

Furthermore, we would like to present the influence of some critical parameters such as dead time, T_d, and P gains, K_P.

Fig. 20 compared the cases in which the dead time are 1 μs (indicated by blue color) and 2.5 μs (indicated by red color), respectively. It is clear to see from Bode plot that the amplitude-frequency response is same but the phase-frequency response has some delays in the larger T_d (2.5 μs) case. This phase delay will result of unstable in the larger T_d (2.5 μs) case.

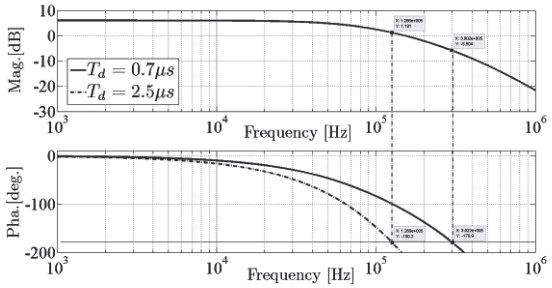

Fig. 20: Effects of dead time in the LLRF system

Fig. 21 compared the cases in which the P gain are 2 (indicated by blue color) and 10 (indicated by red color), respectively. This time the amplitude-frequency response has some difference in the Bode plots. After calculating the gain margin, it is easy to find out that the system will be unstable in the larger K_P case.

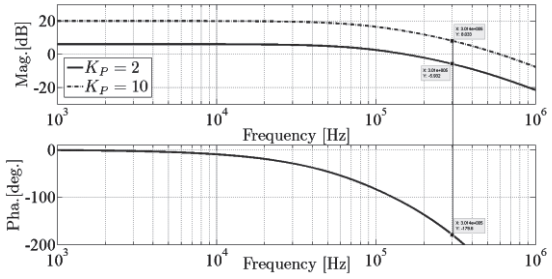

Fig. 21: Effects of PI gains in the LLRF system.

6. LLRF

As mentioned above, the requirement of the LLRF system is to stabilize the RF field inside the RF cavity with some given tolerance. E.g., for cERL LLRF system, the RF field fluctuation should be maintained at less than 0.1% for the amplitude and 0.1 degree for the phase. For future 3 GeV ERL project, this requirement is even tighter (0.01% for the amplitude and 0.01 degree for the phase) [12-15]. Like the general control system, LLRF system also include three basic components: a controller, a plant, and a detector (see Fig. 22). The plant need to control in an LLRF system is usually a cavity (or RF source). For the controller and detector, since the advantages of the digital technologies, new generation LLRF system usually apply the digital devices such as FPGA or/and DSP. In cERL, FPGA-based LLRF system has been developed as well.

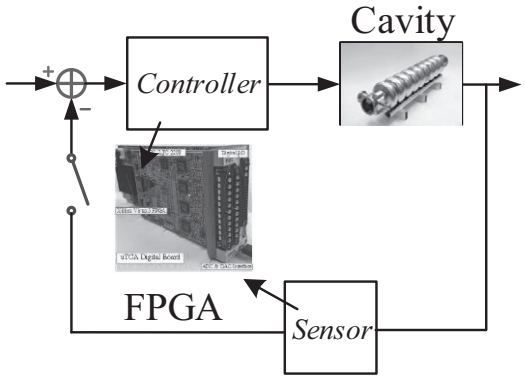

Fig. 22: Components of digital LLRF system.

The FPGA is an integrated circuit that can be programmed in the field after manufacture. Application of FPGA becomes more and more popular in the LLRF field. Since the FPGA is actually a digital devices, however, signals from the RF cavity or RF sources are analog, therefore, the conversion from the analog (digital) to digital (analog) are required. These requirements are fulfilled by analog to digital converter (ADC) and digital to analog converter (DAC). Fig. 23 has illustrated the digital LLRF platform including FPGA, ADC and DAC, this digital platform is applied in the cERL.

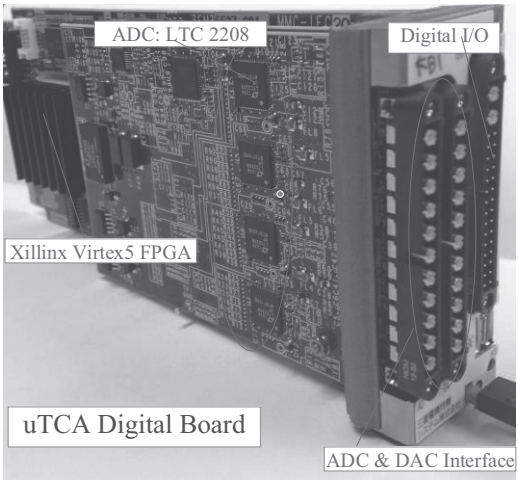

Fig. 23: FPGA in cERL LLRF systems.

6.1. Schematic of LLRF system

A simplified block diagram of the cERL LLRF system is shown in Fig. 25. The 1.3 GHz RF signal (from cavity probe) is down-converted to a 10 MHz intermediate frequency (IF) signal. The IF signal is sampled in the next stage at 80 MHz by a 16-bit analog to digital converter (ADC, LTC2208) and fed into a field-programmable gate array (FPGA).

The base-band in phase and quadrature (I/Q) components are extracted from the digitalized IF signal by a digital I/Q detection model. The notation "I/Q" derives from fact that any sinusoidal signal can be represented by either polar (amplitude/phase) or by Cartesian coordinates. A sinusoidal signal $y(t)$ with amplitude A, radian frequency, ω, and an initial phase ϕ_0, can be decomposed into its sin and cos components by basic trigonometric functions.

$$\begin{aligned} y(t) &= A\sin(\omega t+\phi_0) \\ &= \underbrace{A\cos\phi_0}_{I}\sin(\omega t)+\underbrace{A\sin\phi_0}_{Q}\cos(\omega t) \\ &= I\sin(\omega t)+Q\cos(\omega t) \end{aligned} \quad (6\text{-}1)$$

The amplitude of the sin component and the cos component is then defined as in-phase component (I) and the quadrature-phase component (Q). It is clear to see the relationship between the I/Q and amplitude and phase is given by

$$\begin{cases} I = A\cdot\cos\phi_0 \\ Q = A\cdot\sin\phi_0 \end{cases}, \quad \begin{cases} A = \sqrt{I^2+Q^2} \\ \phi_0 = \arctan(Q/I) \end{cases}. \quad (6\text{-}2)$$

Which means that the amplitude and phase of the RF filed can be represented by the I and Q directly. Fig. 24 has illustrated the mapping between IQ and amplitude and phase [11].

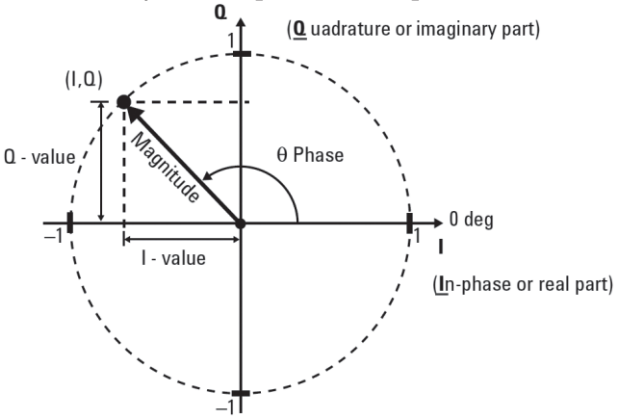

Fig. 24: I/Q vs. amplitude and phase

The I/Q signals are then fed into a 2×2 rotation matrix to correct the loop phase. After being filtered by infinite impulse response (IIR) low-pass filters, the I/Q components are compared to their set values and the IQ errors are calculated. Then, the I/Q errors are regulated by a PI controller. The processed I/Q signals are added to their corresponding FF models. The combinational signals are fed into the I/Q modulator by a 16-bit digital to analog (DAC) converter (AD9783) to modulate the 1.3-GHz RF signal from the oscillator. Finally, the LLRF feedback loop is closed by driving a high-power source, which drives the cavities [12-15].

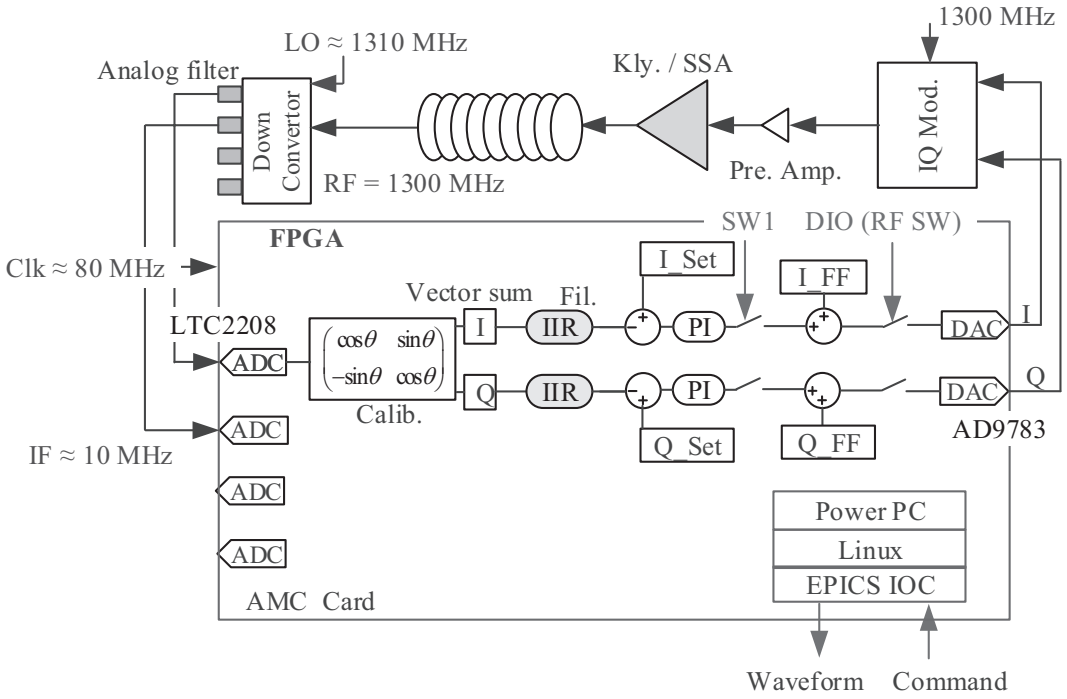

Fig. 25: LLRF system diagram in the cERL at KEK

Some basics features in the LLRF system need to be discussed deeply.

6.2. IQ detection

The I and Q signal was extracted from the IF signals. If the value of the sampling frequency, f_S is four times of the IF frequency ($f_S=4f_{IF}$, aslo named IQ sampling), as shown in upper figure in the Fig. 26. The sequences I, Q, -I, and –Q directly yield. On the other hand as shown in the below figure of Fig. 26, if the relation between f_S and f_{IF} is expressed by [11, 16]

$$f_s = \frac{N}{M} f_{IF} \tag{6-3}$$

In this case, I and Q signal can be calculated by

$$I = \frac{2}{N} \cdot \sum_{k=0}^{N-1} y_i \cdot \cos\left(2\pi k \cdot \frac{M}{N}\right)$$
$$Q = \frac{2}{N} \cdot \sum_{k=0}^{N-1} y_i \cdot \sin\left(2\pi k \cdot \frac{M}{N}\right) \tag{6-4}$$

Sampling method shown in the lower figure of Fig. 26 is also named non-IQ sampling [16].

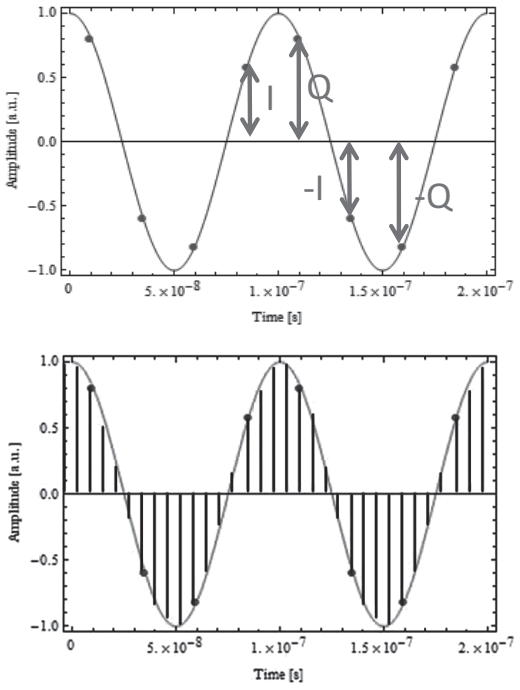

Fig. 26: IQ detection

6.3. PI control and gain-scanning

The digital PI controller, as shown as Fig. 27 is applied in the cERL LLRF system. The transfer function of the PI controller is given by [12-15]

$$H(z) = K_P + \frac{K_I}{1 - z^{-1}} \qquad (6\text{-}5)$$

To determine the optimal PI gains, a gain scanning experiment was carried out in the cERL LLRF system [12-15]. The system performance was measured and evaluated via different proportional gain K_P and integral gain K_I. The measuring procedure comprise the following steps:

- Keep the parameter K_I at a constant value and gradually vary the parameter K_P from 0 to critical gain.
- Measure and record the system performance (the field stabilities with a closed loop) based on a specified (K_I, K_P) pair.
- Update the parameter K_I to a new value after all K_P values are scanned and repeat the procedure 1&2.
- Evaluate the optimal gains according to the measured system performance after all of the K_P and K_I are scanned.

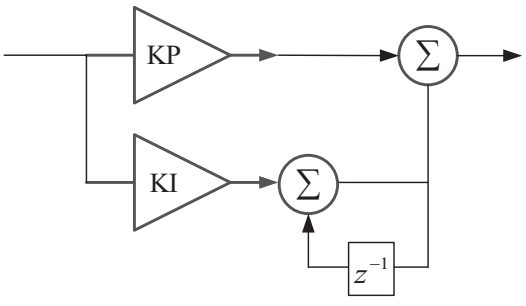

Fig. 27: Digital PI controller.

One of the example of that gain-scanning experiment is given in Fig. 28, the optimum gains are indicated by the white point.

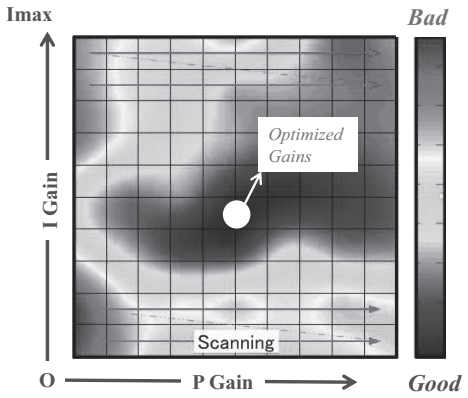

Fig. 28: Gain-scanning experiment.

6.4. Tuner control

Superconducting cavities is subjected to disturbances like microphonics, or Lorentz detuning, that means, the SC cavity do not always worked on resonance, as a result, more RF power is required for a detuned cavity. This problem is resolved by applying for tuner control. The schematic of tuner control is shown in Fig.29. The phase of the cavity probe signal and cavity incident signal are detected, and the phase difference between them is calculated in the next stage. This difference signal is regulated by PI controller. The regulated signal is then send to the DAC for the piezo control and to the digital input/output for the mechanical tuner control. Similar with the LLRF field control, the tuner control is also carried out by another FPGA board.

6.5. Stabilities of LLRF

The typical LLRF system performance and operational parameters during beam commissioning are listed in Table 4. The feedback gains were determined by the gain-scanning experiments, as stated above. Disturbing signals such as microphonics and power supply ripples were suppressed well by the high-gain feedback. The typical RF stabilities of the amplitude and phase, for each

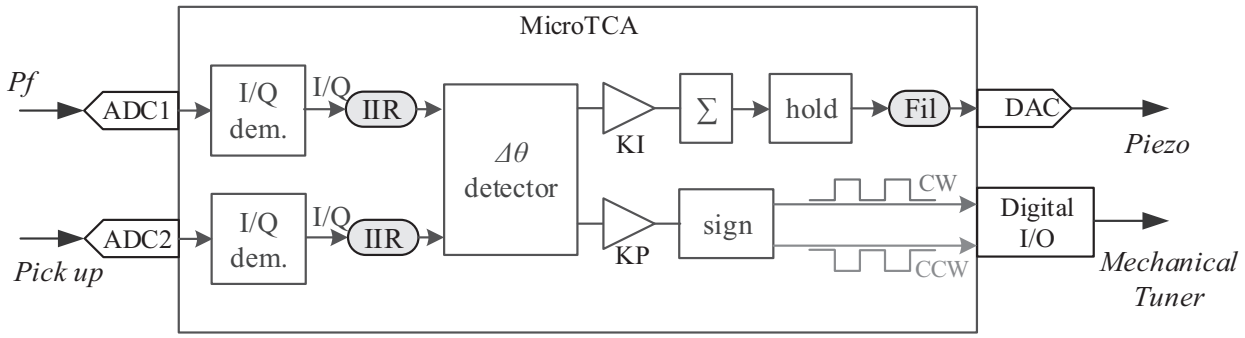

Fig. 29: Schematic of Tuner control.

cavity in the main linac and injector were given in Fig. 30 and Table 4 [12-15]. As stated above, our requirement for the cERL LLRF systems are 0.1% for amplitude and 0.1 degree for phase. Results in Fig. 30 and Table 4 indicate that these requirement is satisfied by the FPGA-based LLRF system in compact ERL.

Table 4 Stabilities of LLRF system

Cavity	φ_b	V_c	RF stability (rms)	
			$\delta A/A$	$\delta\theta$
Buncher	-90°		0.07%	0.04°
Inj. 1	0°	0.7 MV	0.006%	0.009 °
Inj. 2	0°	0.65 MV	0.007%	0.025°
Inj. 3	0°	0.65 MV		
ML1	0°	8.56 MV	0.003%	0.010°
ML2	0°	8.56 MV	0.003%	0.007°

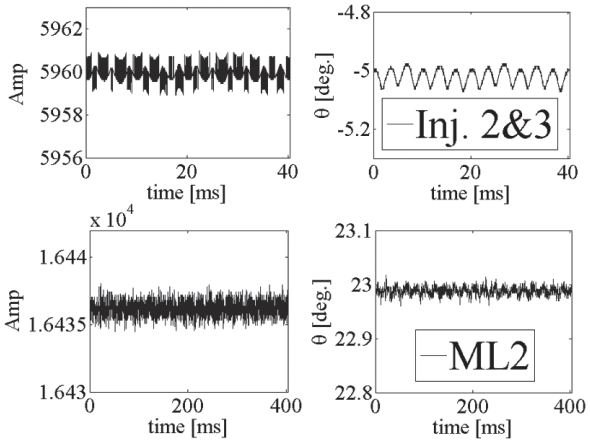

Fig. 30 Stabilities of LLRF system.

7. Stability of beam current

The beam energy stability is measured by the screen monitor which is installed downstream of the bending magnet with a 2.2 m dispersion and 62.6 μm/pixel resolution [13]. The beam momentum jitter is calculated based on the peak point of the beam projection in the screen monitor. The calibrated beam momentum jitter is about 0.006% rms as shown in Fig. 31 This value is in consistence with the measured RF stability in the LLRF system.

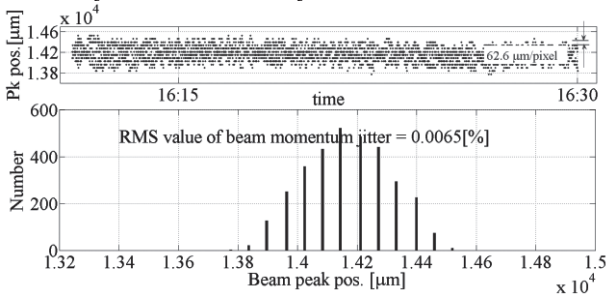

Fig. 31: Beam energy stability in the cERL.

8. Summary

In this speech, we have introduced the RF system at first, we present the main components of an RF system. Furthermore, we have discussed several main RF sources in the cERL. In addition, we have presented the basic issue of the control theory and LLRF system, finally we gives the performance of the RF system in cERL.

Reference

[1] CERN accelerator school on RF engineering, Seeheim, Germany, 8-16 May 2000.

[2] CERN Accelerator School on RF for accelerators, Ebeltoft, Denmark, 8-17 June 2010.

[3] A. Jain, et al, Compact solid state radio frequency amplifiers in kW regime for particle accelerator subsystems. Sadhana Vol. 38, Part 4, August 2013, pp. 667–678.

[4] Jorn Jacob, RF Solid State Amplifiers, CAS-CERN Acclerator School, Baden, 7-14 May 2014 (https://cas.web.cern.ch/cas/Switzerland-2014/Lectures/Jacob.pdf)

[5] R. Heppinstall, et. al, The inductive output tube. The latest generation of amplifier for digital terrestrial television transmission.

[6] Microwave components and circuits. (http://www.navymars.org/national/training/nmo_courses/nmo1/module11/14183_ch2.pdf)

[7] Rebecca Seviour, et. al, Comparative Overview of Inductive Output Tubes, June 2011.

[8] H. Bohlen, et. al, IOT RF Power Sources for Pulsed and CW Linacs, LINAC 2004.

[9] F. Qiu, et. al, A disturbance-observer-based controller for LLRF systems, proceedings of IPAC2015, Richmond, USA, 2015

[10] https://en.wikipedia.org/wiki/Control_system

[11] T. Schilcher, Digital signal processing in RF applications, CERN accelerator school on digital signal processing, Sigtuna, Sweden, May 2007.

[12] F. Qiu, et al., Evaluation of the superconducting LLRF system at cERL in KEK, IPAC2013, Shanghai, May 2013.

[13] F. Qiu, et al., Digital filters used for digital feedback system at cERL, LINAC14, Geneva, Switzerland, 2014

[14] F. Qiu, Performance of CW Superconducting Cavity at ERL test facility, LLRF2013 workshop, Lake Tahoe, California, US, 2013

[15] F. Qiu, et al., Performance of the Digital LLRF System at the cERL, IPAC'14, Dresden, June, 2014

[16] S. simrock, Z. Geng, Cavity field control, RF signal detection and actuation, 8th International Accelerator School for Linear Colliders (https://agenda.linearcollider.org/event/6258/contribution/27/material/slides/3.pdf)